*ACTA ASTRONOMICA*
Vol. **66** (2016) pp. 197–217

# OGLE Study of the Sagittarius Dwarf Spheroidal Galaxy and its M54 Globular Cluster*

A. Hamanowicz[1], P. Pietrukowicz[1], A. Udalski[1], P. Mróz[1], I. Soszyński[1], M.K. Szymański[1], J. Skowron[1], R. Poleski[1,2], Ł. Wyrzykowski[1], S. Kozłowski[1], M. Pawlak[1] and K. Ulaczyk[1,3]

[1] Warsaw University Observatory, Al. Ujazdowskie 4, 00-478 Warszawa, Poland
e-mail:(ahamanowicz,pietruk,udalski)@astrouw.edu.pl
[2] Department of Astronomy, Ohio State University, 140 W. 18th Ave., Columbus, OH 43210, USA
[3] Department of Physics, University of Warwick, Gibbet Hill Road, Coventry, CV4 7AL, UK

*Received May 11, 2016*

ABSTRACT

We use the fundamental-mode RR Lyr-type variable stars (RRab) from OGLE-IV survey to draw a 3D picture of the central part of the tidally disrupted Sagittarius Dwarf Spheroidal (Sgr dSph) galaxy. We estimate the line-of-sight thickness of the Sgr dSph stream to be $\mathrm{FWHM_{cen}} = 2.42$ kpc. Based on OGLE-IV observations collected in seasons 2011–2014 we conduct a comprehensive study of stellar variability in the field of the globular cluster M54 (NGC 6715) residing in the core of this dwarf galaxy. Among the total number of 268 detected variable stars we report the identification of 174 RR Lyr stars, four Type II Cepheids, 51 semi-regular variable red giants, three SX Phe-type stars, 18 eclipsing binary systems. Eighty-three variable stars are new discoveries. The distance to the cluster determined from RRab stars is $d_{\mathrm{M54}} = 26.7 \pm 0.03_{\mathrm{stat}} \pm 1.3_{\mathrm{sys}}$ kpc. From the location of RRab stars in the period–amplitude (Bailey) diagram we confirm the presence of two old populations, both in the cluster and the Sgr dSph stream.

**Key words:** *Galaxies: individual: Sgr dSph – globular clusters: individual: M54 (NGC 6715) – Stars: variables: RR Lyr – Cepheids*

## 1. Introduction

The Sagittarius Dwarf Spheroidal (Sgr dSph) galaxy, discovered by Ibata *et al.* (1994), is a tidally disrupted stellar system colliding with the Milky Way. Streams of this dwarf galaxy are extended around in the sky (Majewski *et al.* 2003, Belokurov *et al.* 2006, Torrealba *et al.* 2015). Studies of the spatial location of the streams help to test models of the dark matter distribution in our Galaxy (Belokurov *et al.* 2014).

---

*Based on observations obtained with the 1.3-m Warsaw telescope at the Las Campanas Observatory of the Carnegie Institution for Science.

Globular cluster M54 is considered to be the actual core of the Sgr dSph galaxy. It is located at the Galactic coordinates $(l,b) = (+5\overset{\circ}{.}607, -14\overset{\circ}{.}087)$. However, the question where this cluster was formed remains open. Photometric observations conducted in 1990s by Sarajedini and Layden (1995) and also Layden and Sarajedini (1997) indicated that M54 is physically associated with the Sgr dwarf. Later studies by Majewski *et al.* (2003) and Monaco *et al.* (2005) demonstrated that there is a nuclear condensation in the Sgr system independent of the presence of the metal-poor population identified with the globular cluster M54. Bellazzini *et al.* (2008) compared radial velocities of 1152 candidate red giant branch stars from Sgr dSph and M54, obtaining significantly different velocity dispersion profiles in both systems. They concluded that the actual Sgr dSph nucleus was most likely formed independently of M54. Searches for variable stars, particularly RR Lyr-type stars being tracers of old populations, may help in the determination of physical parameters and better understanding of the formation process of M54 and the whole Sgr dSph stream (*e.g.*, Kunder and Chaboyer 2009, Zinn *et al.* 2014).

First wide-field searches for RR Lyr stars in the main part of the Sgr dSph galaxy were undertaken by the Optical Gravitational Lensing Experiment (OGLE) and Disk Unseen Objects (DUO) surveys, already in the year in which the dwarf galaxy was discovered. Mateo *et al.* (1995ab) reported seven RR Lyr stars from the OGLE-I survey, very likely members of the Sgr dSph, and estimated the distance to the dwarf of $25.2 \pm 2.8$ kpc assuming a RR Lyr absolute brightness of $M_V = +0.6$ mag. Later, Cseresnjes *et al.* (2000) presented the discovery of about 1500 fundamental-mode (RRab) pulsators in a 50 deg$^2$ area of the Sgr dwarf monitored by DUO. Based on averaged periods obtained for RRab and also RRc (first-overtone) pulsators Cseresnjes (2001) placed the Sgr dSph galaxy in the long-period tail of the Oosterhoff I (OoI) group. From the period and amplitude distributions of the RR Lyr population they found an average metallicity of $[\mathrm{Fe/H}] = -1.6$ dex with a contribution of a minor population with [Fe/H] below $-2$ dex. At the same time, metallicity gradients were noticed by Alard (2001) who compared red giant branches in two fields separated by $6^\circ$ along the Sgr dSph stream. Similar findings were announced by Zinn *et al.* (2014) who surveyed about 840 deg$^2$ of the Galactic halo including the Sgr dSph stream: RRab stars belonging to the stream form a mixture of OoI and OoII groups with heavy weight toward OoI. From 208 RRab variable stars observed by the MACHO survey (Alcock *et al.* 1997) and associated with the Sgr dSph galaxy Kunder and Chaboyer (2009) derived the distance to its northern extension. They obtained $24.8 \pm 0.8$ kpc and concluded that the extension of the Sgr dSph galaxy toward the Galactic plane is inclined toward us.

Recently, Soszyński *et al.* (2014) reported the detection of 2286 RR Lyr variable stars in a 9.8 deg$^2$ area toward the main body of the Sgr dwarf surveyed by the OGLE-IV project (Udalski *et al.* 2015). Among the variables there are 1767 RRab, 499 RRc, and 20 RRd (double-mode) type stars.

First variable stars in the field of M54 globular cluster were discovered by Rosino (1952) who photographically found 28 such objects. Among them there were two Type II Cepheids and 15 candidate RR Lyr-type stars. Later, Rosino and Nobili (1958) reported on another 54 variable stars, almost all of them of RR Lyr type. A search for variable stars conducted by Layden and Sarajedini (2000) provided 35 new objects, roughly half of which are RR Lyr stars and the other half are variable red giants. Other, more recent studies include Sollima *et al.* (2010) work who announced the discovery of 94 new variable stars and Montiel and Mighell (2010) reanalysis of archival Hubble Space Telescope (HST) Wide Field Planetary Camera 2 (WFPC2) images of the center of the cluster. They reported 50 candidates for RR Lyr stars. The HST observations were obtained in 1999 and consist of six images in the F814W filter (close to the standard *I* passband) and six images in the F555W filter (*V* passband) spanning 7.5 hours total. Fourteen of the proposed candidates can be assigned to the previously known variable stars. The whole list of variable stars in the field of M54 is presented in Clement *et al.* (2001) who made an on-line update in 2014[†]. Three-fourths of all variable stars in this list are RR Lyr stars.

In recent years, two independent distance indicators were used to measure the distance to the globular cluster M54: RR Lyr variable stars and tip of the red giant branch (TRGB) stars. The following distance estimates can be found in the literature: $27.4 \pm 1.5$ kpc (Layden and Sarajedini 2000, based on RR Lyr stars), $26.30 \pm 1.8$ kpc (Monaco *et al.* 2004, TRGB stars), $26.7 \pm 1.1$ kpc (Sollima *et al.* 2010, RR Lyr stars). According to the 2010 update of the Harris (1996) catalog, the center of M54 is located at $(\alpha,\delta)_{2000.0} = (18^{\rm h}55^{\rm m}03\overset{\rm s}{.}33,\ -30^{\circ}28'47\overset{\prime\prime}{.}5)$, the globular cluster has the core radius $r_{\rm c} = 0\overset{\prime}{.}09$ and half-light radius $r_{\rm h} = 0\overset{\prime}{.}82$. The cluster tidal radius $r_{\rm t}$ is estimated to be about $7\overset{\prime}{.}5$, according to the first edition of this catalog.

In this work, based on all detected RRab stars in the OGLE-IV Galactic bulge fields we draw a 3D picture of the Sgr dSph galaxy in the background of the old Milky Way bulge (Pietrukowicz *et al.* 2015). We estimate the line-of-sight thickness of the Sgr stream. We also search for any type of variable objects within the tidal radius of M54 using observations spanning four-years from the OGLE-IV survey and by applying non-standard reduction techniques. Based on RRab stars we determine the distance to M54. Finally, using period–amplitude diagram, we compare distributions of this type of stars residing in the core cluster with properties of RR Lyr stars from the Sgr dSph galaxy.

It is worth noting that results of an independent search for variable objects in the very central part of M54 (Figuera Jaimes *et al.* 2016) have recently been announced almost simultaneously with the presented here discoveries.

[†] *http://www.astro.utoronto.ca/~cclement/read.html*

## 2. Observations

The OGLE project is the worldwide largest stellar variability sky survey, with one trillion ($10^{12}$) single brightness measurements collected and nearly half a million genuine variable stars discovered by 2016. The survey is conducted at Las Campanas Observatory, Chile, since 1992. OGLE monitors about 1.3 billion stars in the sky toward the Milky Way bulge and disk and the Magellanic System in searches for periodic as well as transient objects (*e.g.*, Soszyński *et al.* 2013, 2014, 2015, Pietrukowicz *et al.* 2013, Mróz *et al.* 2015). For over 20 years OGLE operates the dedicated 1.3-m Warsaw telescope. Since 2010 the project is in its fourth phase, OGLE-IV. The OGLE-IV camera is a mosaic of 32 $2\text{K}\times4\text{K}$ CCDs giving a total field of view of 1.4 $\text{deg}^2$ at the scale of 0.26 arcsec/pixel. Most of images (about 90%) are taken in the *I*-band filter, while the remaining images are taken in the *V*-band filter. Detailed description of the OGLE-IV survey, instrumentation and data reduction can be found in Udalski *et al.* (2015).

During 2011–2014, OGLE observed seven fields (BLG705–BLG711) toward the main part of the Sgr dSph galaxy. For each of the seven fields about 160 *I*-band and 10 *V*-band frames were collected, all with exposure times of 150 s. Most of the *I*-band data were obtained in 2011. The distribution of the OGLE-IV Galactic bulge fields with detected RR Lyr stars are presented in Soszyński *et al.* (2014). These observations constitute a pilot study of the part of Sgr dSph stream crossing the Milky Way. Currently, the OGLE project conducts a variability survey of the outer Galactic bulge, including a much larger area of the Sgr dSph stream (see Fig. 3 in Pietrukowicz 2016).

## 3. 3D Picture of the Sgr dSph Galaxy

### *3.1. Distance Estimation from RR Lyr Stars*

RR Lyr variable stars are very useful distance indicators. Particularly, RRab stars have several advantages over other types of these pulsators. In comparison to RRc (and also very rare RRd) stars, RRab variable stars are more numerous, on average are intrinsically brighter in *I*, have higher amplitudes, and have characteristic saw-tooth-shaped light curves, making the searches highly complete. There is one more very practical photometric property of RRab stars: based on the pulsation period $P$ and a combination of Fourier decomposition phases $\phi_{31} = \phi_3 - 3\phi_1$ of a star one can estimate its metallicity [Fe/H] (Jurcsik 1995, Jurcsik and Kovács 1996). Recently, RRab stars from OGLE-IV have been used by Pietrukowicz *et al.* (2015) to study three-dimensional structure of the old Galactic bulge. Here, we apply a similar approach to determine distances to the RRab variable stars laying between the half-light and tidal radii of the globular cluster M54 and other RR Lyr variable stars in the Sgr dSph area observed by OGLE-IV (fields BLG705–BLG711). We use the following sequence of equations to derive physical properties and distance

$d$ to the individual RRab stars:

$$
\begin{aligned}
[\mathrm{Fe/H}] &= -3.142 - 4.902\,P + 0.824\,\phi_{31}, & (1)\\
\log Z &= [\mathrm{Fe/H}] - 1.765, & (2)\\
M_I &= 0.471 - 1.132\log P + 0.205\log Z, & (3)\\
M_V &= 2.288 + 0.882\log Z + 0.108(\log Z)^2, & (4)\\
(V-I)_0 &= M_V - M_I, & (5)\\
E(V-I) &= 1.375\,E(B-V), & (6)\\
A_I &= 1.969\,E(B-V), & (7)\\
I_0 &= I - A_I, & (8)\\
d &= 10^{1+0.2(I_0-M_I)}. & (9)
\end{aligned}
$$

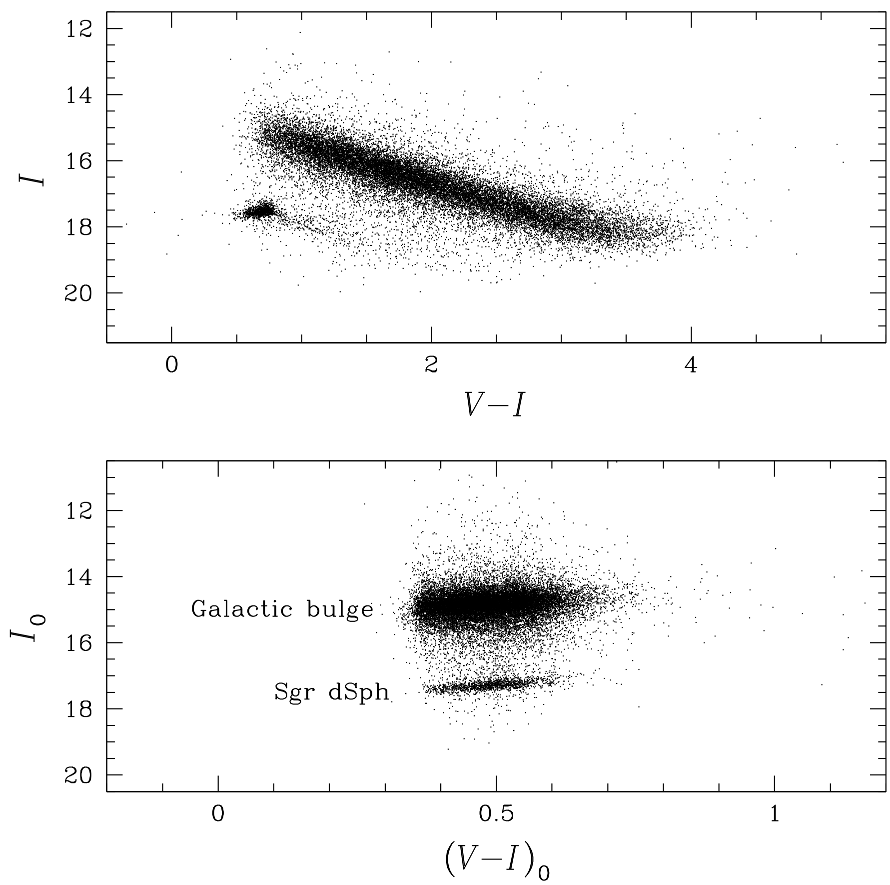


Fig. 1. Observed (*upper panel*) and dereddened (*lower panel*) CMDs for RRab stars in the OGLE-IV bulge fields. Sgr dSph stars clearly separate from the Galactic bulge variable stars.

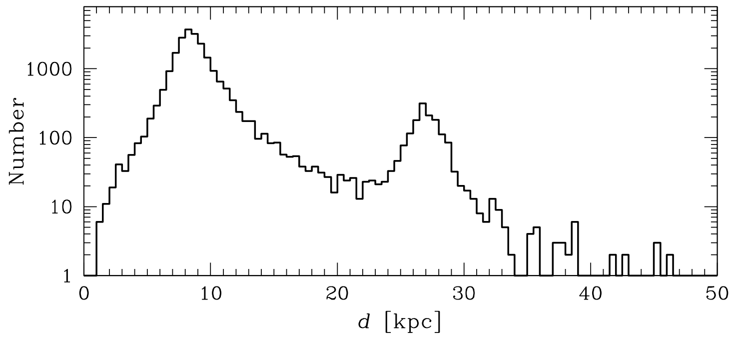


Fig. 2. Distance distribution for about 22 900 RRab stars observed in the OGLE-IV Galactic bulge fields. The maxima correspond to the Galactic bulge and roughly three times more distant Sgr dSph galaxy. The sharp peak for the Sgr dwarf is mainly formed by the variable stars from the globular cluster M54.

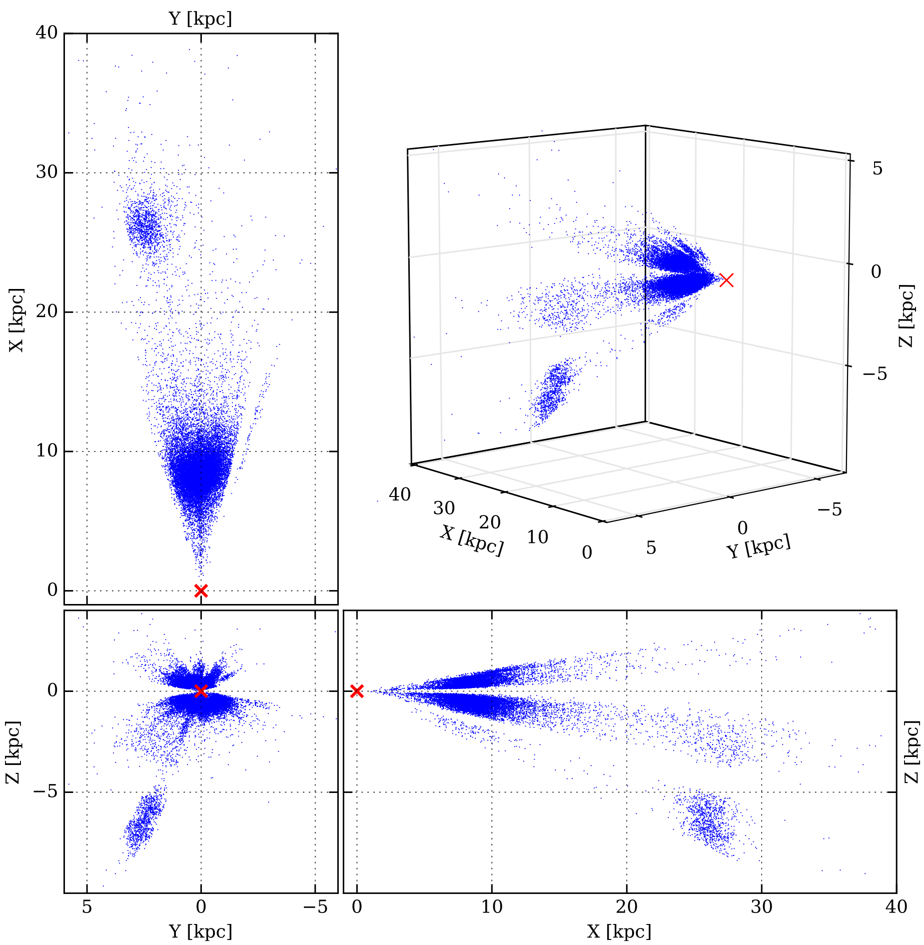


Fig. 3. Distribution of about 22 900 OGLE RRab stars in 3D space with the origin in the Sun (marked with red cross). Most of the stars are Galactic bulge objects. The second prominent structure is the Sgr dSph galaxy.

We use the empirical relation on metallicity (Eq. 1) derived for $I$-band light curves by Smolec (2005). Relations on the absolute brightnesses $M_I$ and $M_V$ (Eqs. 3–4 together with Eq. 2) come from the theoretical work by Catelan *et al.* (2004). Reddening values $E(B-V)$ were taken from the extinction map in Schlegel *et al.* (1998), corrected by a factor of 0.86 as suggested by Schlafly and Finkbeiner (2011), and transformed to $E(V-I)$ and $A_I$ using extinction-law coefficients from Schlegel *et al.* (1998). In Fig. 1, we present observed and dereddened CMDs for about 22 900 OGLE RRab variable stars with measured brightnesses in $V$ and $I$. In Fig. 2, we show histogram of the obtained distances to these stars. Fig. 3 presents the 3D distribution of all RRab variable stars. The origin of the coordinate system is in the Sun and the $X$ axis points toward the Galactic center. Variable stars from the Sgr dSph galaxy form a prominent group behind the Galactic bulge, but they are mixed with Galactic halo and thick disk stars.

### *3.2. Thickness of the Sgr dSph Stream*

In Fig. 4, we present the results of estimating thickness of the Sgr dSph stream in two observed directions: toward its core section and behind the Galactic bulge. What we determine is the full width at half maximum FWHM $\approx 2.35\sigma$ of a Gaussian profile fitted to the histogram of derived in Section 3.1 RR Lyr distances. In the central section the observed FWHM is 2.49 kpc. Variable stars from the globular cluster M54 were not taken into account for this measurement. The part of the Sgr dwarf behind the Galactic bulge is clearly superimposed on the declining distribution of the Galactic halo and thick disk RR Lyr stars. In this direction, the stream seems to be thicker with the observed FWHM of 3.50 kpc (after correction for Galactic background; *cf.* Fig. 4 – middle panel). To obtain the true FWHM of the Sgr stream, from the observed value we need to quadratically subtract FWHM corresponding to the statistical uncertainty of the distance, $2.35\sigma_{\rm d}$. If we adopt a mean accuracy of OGLE brightness measurements of $\sigma_I = 0.02$ mag, for the Sgr central section we find an uncertainty of the distance $\sigma_{\rm d} \approx 0.25$ kpc, hence $\mathrm{FWHM_{cen}} \approx 2.42$ kpc. For the section behind the bulge, for which we use the $E(J-K_s)$ map from Gonzalez *et al.* (2012) with statistical $\sigma_{\rm E(J-Ks)} \approx 0.01$ mag, we find an uncertainty of the distance modulus of 0.040 mag ($\sigma_{\rm d} \approx 0.5$ kpc) and the true $\mathrm{FWHM_{offcen}} = 3.30$ kpc.

Comparison of the distances in the two directions do not favor the result from Kunder and Chaboyer (2009) that the Sgr stream is inclined toward us closer to the Galactic plane. However, one has to remember that our sample of Sgr dwarf variable stars at lower Galactic latitudes is incomplete due to high reddening close to the Galactic plane. Moreover, we applied different dereddening procedures for objects located at $b < -10^\circ$ (updated map from Schlegel *et al.* 1998) and $b > -10^\circ$ (relation on extinction from Nataf *et al.* 2013).

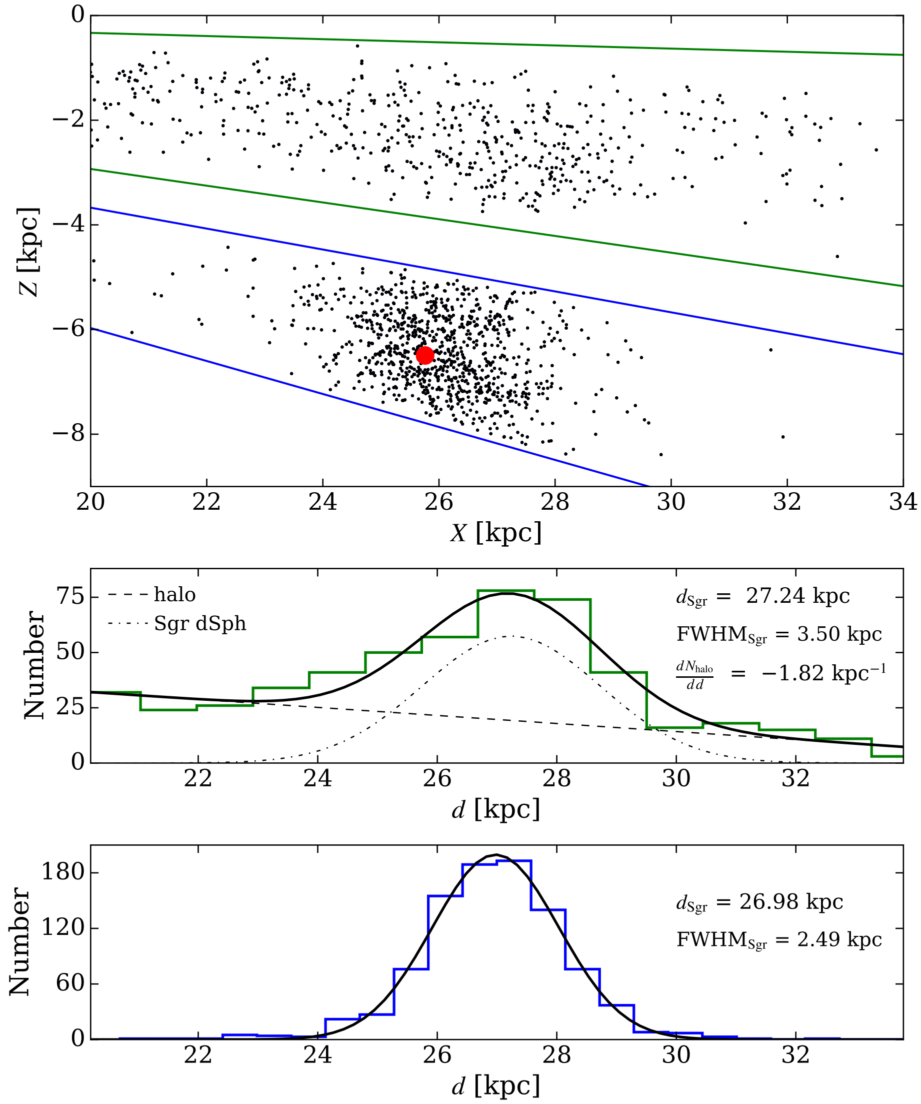


Fig. 4. Distance and observed line-of-sight thickness of the Sgr dSph stream. The *upper panel* shows RRab stars in the projection onto the $XZ$ plane. The Sun and Galactic Center (GC) are on the left-hand side of *this panel*. Red circle marks the exact position of the globular cluster M54 as found in Section 6. Histograms in the *middle panel* and *lower panel* show the distance distributions in two directions delimited by green and blue lines, respectively.

## 4. Search for Variable Stars in the Field of M54

The center of the globular cluster M54 can be found in the northern part of the CCD #09 in the OGLE field BLG708. The cluster half-light area is well within this CCD, but the whole area delimited by the tidal radius partially spans also over CCDs #08, 10, 17, 18, and 19 in the same field. Location of the OGLE CCDs together with location of the HST/WFPC2 detectors is shown on the map of detected RRab stars in Fig. 5. About 3.9% of the whole cluster area falls in the gaps between the OGLE CCDs.

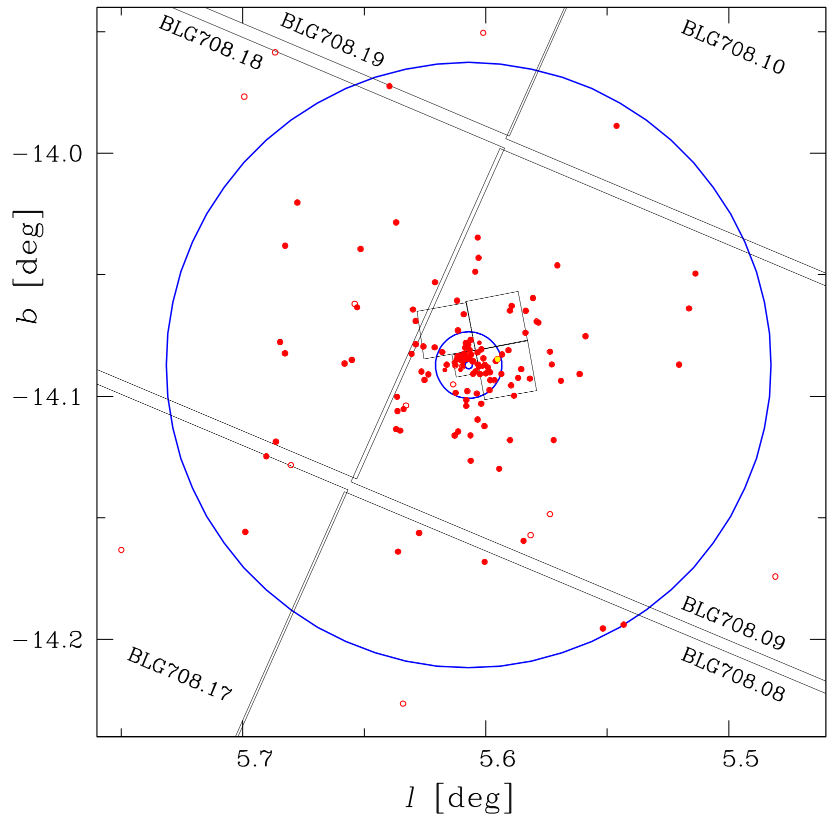


Fig. 5. RRab stars in the field of the globular cluster M54. Blue circles represent the characteristic cluster radii: core (0′.09), half-light (0′.82), and tidal (7′.5). Long black lines delimit the OGLE-IV chips. Central black squares show the area observed with the HST/WFPC2 camera. RRab stars belonging to the cluster are marked with filled red circles, while field stars are marked with empty circles. The unusually long-period RRab variable V92, located approximately at half-light radius, is marked with a yellow circle. All RRab stars located outside the tidal radius were classified as field objects.

The search for variable stars was done in three stages. In the beginning, we searched for any kind of variable objects among stars detected with the standard OGLE reduction pipeline which is based on the image subtraction technique (*cf.* Udalski *et al.* 2015). We limited ourself to objects detected within the tidal radius of the cluster. All light curves were then subject to the period search. We used OGLE standard periodogram procedure – FNPEAKS Fourier analysis software‡, providing the most prominent periods and their signal-to-noise.

‡*http://helas.astro.uni.wroc.pl/deliverables.php?lang=en&active=fnpeaks*

We made a visual inspection of *I*-band light curves of 4711 detections with a significant periodicity signal $(\mathrm{S}/\mathrm{N} > 4)$ selected from a total number of 53 297 point sources. After rejection of some false identifications due to blending and crowding, particularly strong in the inner part of the cluster, 192 candidate variable stars were left. Then, we identified the OGLE counterparts with variable objects in the updated Clement *et al.* (2001) list. The identification was generally based on coordinates, but also on observed brightness and variability time-scales. We found 24 objects to be non-variable at all and eight variable stars misclassified. Thanks to the long-term OGLE observations we could obtain more accurate periods for pulsating variable stars and eclipsing binary stars. Relative period uncertainties for these types of periodic variable stars are usually between $10^{-6}$ and $10^{-5}$, as returned by the TATRY code (Schwarzenberg-Czerny 1996). In the case of semi-regular variable red giants, errors of estimated periods are of 1 d or larger.

We also verified, yet unconfirmed, candidates for RR Lyr stars found by Montiel and Mighell (2010) in the archival HST/WFPC2 images of the central area of M54 (program GO 6701). Ten of the stars located in moderately crowded regions were easily cross-matched with the OGLE detections. In the case of the remaining objects, we encountered a problem of the lack of any detections from the standard OGLE image reduction pipeline. It was a result of generating $11 \times 11$ pixel masks in the location of bright stars with over 60 000 counts per pixel to secure linear transformation to magnitudes. We found that the brightest stars in the center of M54 did not in fact reach the saturation limit of 65 536 counts in our frames and crossed the 60 000 limit in just single pixels.

In this situation, we decided to perform a second stage of variable stars search by reducing in a different way the data for a central 3.0 arcmin$^2$ area. First, we lowered the mask size to only one pixel. We chose eleven difference images with the lowest seeing. Then, after taking the absolute value of all residuals we stacked the images together creating a variability image. In such a combined image, the signal from variable sources was expected to be much stronger. Searches for positive detections resulted in finding of 2730 candidate variable sources. In the position of each source, we extracted *I*-band time-series photometry. After visual inspection of the new light curves, rejection of false positives, and cross-matching with the updated Clement *et al.* (2001) list, we were left with 85 variable objects.

Positions of only three objects coincided with the positions of unconfirmed candidate RR Lyr stars from HST (Montiel and Mighell 2010). Among other sources we found 14 new RR Lyr type stars and two new Type II Cepheids. All variable stars were calibrated from the instrumental to the standard magnitudes using transformation relations and coefficients given in Udalski *et al.* (2015). In the case of several new variable stars, we assumed the average color of other variable stars of the same type due to severe crowding and lack of *V*-band information.

Finally, as a third stage, we decided to extract OGLE *I*-band photometry in the exact locations of all 50 HST candidate RR Lyr stars. Prior to that we reduced the archival WFPC2 images using the HSTPHOT package (Dolphin 2000ab). We performed some initial image processing steps like masking bad pixels and cosmic-ray rejection. Profile photometry was obtained using a library of model point-spread functions and transformed to the standard *V* and *I* bands using the utility available in the HSTPHOT package. $(X,Y)$ positions of candidates on the HST images were transformed to the $(X,Y)$ grid of the OGLE reference image to allow photometry at correct position on the OGLE difference images. If the resulting light curve contained periodic signal in the suitable period range and the shape resembled that of RR Lyr stars the detection was considered as positive.

We confirm the presence of another seven RR Lyr stars and assess their periods based on the OGLE data. It should be stressed here that neither of the new RR Lyr stars could be clearly resolved on the OGLE reference image due to severe crowding in the central part of the cluster in spite of its good resolution of $\approx 1''$. Nevertheless, the difference signal was sound in all these cases.

Unfortunately, we are not able to detect any variability signal at the positions of the remaining 16 candidates (50 minus 14 cross-identified with the Clement's *et al.* list minus 20 detected during our search in stages 1–3) indicated by Montiel and Mighell (2010) in the HST/WFPC2 images. To calibrate the confirmed RR Lyr variable stars we scaled and shifted the phased OGLE *I*-band light curves to match the brightness returned by HSTPHOT. Due to severe crowing in the central part of the cluster the accuracy of zero points for these stars can be as bad as 0.1 mag.

Summarizing, our search for variable stars in the M54 cluster field led to the discovery of 83 new variable stars. We also cross-identified and verified 205 objects from the Clement's *et al.* (2001) list of M54 variable objects containing 211 stars. We also note that there is no OGLE photometry for variables V14, V56, V65, V66, V108, and V157. These stars fell in the gaps between the OGLE CCDs.

## 5. Detected Variable Stars

The final list of variable stars in the field of the globular cluster M54, time-series *V*- and *I*-band photometry and finding charts are available to the astronomical community from the OGLE Internet Archive:

*http://ogle.astrouw.edu.pl*
*ftp://ftp.astrouw.edu.pl/ogle/ogle4/OCVS/M54/*

Originally, we planed to continue Clement's *et al.* (2001) scheme of numbering the variable stars by assigning the name "V212" (the first available new variable) to our first variable and so on. In the first publicly available version of our paper such numbering was presented. However, because the results of independent search for variable stars in the central regions of M54 conducted by the MiNDSTEp consortium were published practically simultaneously with our results (Figuera Jaimes *et al.* 2016) and they introduced similar to our numbering scheme of their variable objects we jointly undertook efforts to synchronize the naming convention to avoid ambiguities and confusion for the future researchers working on the globular cluster M54.

We decided to rename the original OGLE names and assign names V212 to V291 for objects presented in the MiNDSTEp paper (Table 3, Figuera Jaimes *et al.* 2016). The remaining OGLE new variable stars – not present on the MiNDSTEp list – follow as variable stars V292–V347. However, one has to remember that 46 out of 76 MiNDSTEp objects (V212–V291) were also found in this study and these are independent discoveries.

Figuera Jaimes *et al.* (2016) used Electron-Multiplying CCD detector and technique allowing obtaining much better image resolution, thus they were able to search for variable stars in the most dense part of M54, practically not accessible for the standard OGLE observing setup. Most of the OGLE missing variable stars are located in the very center of the cluster.

For 20 RR Lyr stars from the HST candidate list (Montiel and Mighell 2010) confirmed as genuine pulsating stars in this OGLE study, 16 have been also listed by MiNDSTEp. We assign IDs from V292 to V295 for the remaining 4. Other newly discovered variable stars have numbers from V296 to V347 and are sorted with increasing right ascension. In the file listing the variable stars (M54variables.dat in the OGLE Internet Archive), we provide for each object information on coordinates, distance from the center of the cluster, variability type, detected period, *V*- and *I*-band brightnesses, and *I*-band amplitude, if available. Remarks on some stars are given in the last column.

We confirm that objects already marked by Clement *et al.* (2001) as constant stars do not show any brightness variations, *i.e.,* positions: V20, V21, V22, V24, V26, V27, V53, V72, and V100. Surprisingly, 28 variable stars (mostly classified as RR Lyr-type stars) do not vary at all. These are objects: V73, V79, V81, V86, V91, V107, V155, V166, V167, V169, V170, V175, V189, V195, V196, V197, V198, V199, V200, V201, V202, V203, V204, V205, V207, V208, V209, and V211. Among objects from V190 to V211 reported by Sollima *et al.* (2010), fifteen are in fact very bright constant stars located at a distance of a few $r_{\rm h}$ from the cluster center. Several objects from V196 to V210 had very suspicious periods that closely grouped either around a value of 0.35 d or 0.50 d. Bright objects (with $I \approx 13$ mag) named V190, V191, V206, and V210 are not RR Lyr-type stars but variable red giants. The same conclusion refers to variable V71.

We confirm that Soszyński *et al.* (2014) correctly classified variable V12 as a RRd star. They also correctly identified variables V172, V184, and V192 as RRab stars, not RRc stars as it had been thought before. These three variable stars have light curves typical for RRab stars and pulsation periods longer than 0.6 d. For a comparison, RRc type stars have pulsation periods in the range between 0.20 d and 0.54 d.

Among RR Lyr stars discovered by Soszyński *et al.* (2014), 19 variable stars are located within the M54 tidal radius and are not included in the updated list by

Clement *et al.* (2001). These are stars:
V227=OGLE-BLG-RRLYR-37582, V228=OGLE-BLG-RRLYR-37575, V229=OGLE-BLG-RRLYR-37597, V233=OGLE-BLG-RRLYR-37591, V236=OGLE-BLG-RRLYR-37585, V237=OGLE-BLG-RRLYR-37570, V240=OGLE-BLG-RRLYR-37576, V244=OGLE-BLG-RRLYR-37581, V246=OGLE-BLG-RRLYR-37573, V250=OGLE-BLG-RRLYR-37590, V251=OGLE-BLG-RRLYR-37579, V252=OGLE-BLG-RRLYR-37593, V253=OGLE-BLG-RRLYR-37586, V295=OGLE-BLG-RRLYR-37578, V296=OGLE-BLG-RRLYR-37500, V310=OGLE-BLG-RRLYR-37565, V321=OGLE-BLG-RRLYR-37594, V330=OGLE-BLG-RRLYR-37621 and V338=OGLE-BLG-RRLYR-37662. Variable V321 is the second known RRd type star in M54.

Among the 50 HST candidates for RR Lyr variable stars proposed by Montiel and Mighell (2010), 14 stars were indeed known before as noticed by C. Clement: V127=VC2, V162=VC11, V163=VC12, V95=VC13, V164=VC14, V142=VC15, V129=VC17, V179=VC18, V181=VC28, V160=VC34, V46=VC44, V148=VC45, V192=VC46, and V76=VC47. With the OGLE photometry we confirm that the following 20 variable stars are RR Lyr stars: V213=VC40, V214=VC39, V215=VC25, V220=VC4, V223=VC10, V231=VC26, V233=VC30, V234=VC7, V236=VC36, V237=VC31, V241=VC1, V250=VC23, V255=VC5, V284=VC32, V285=VC33, V291=VC27, V292=VC16, V293=VC22, V294=VC24, and V295=VC38. Five of the stars, namely V213, V215, V291, V292, and V294, turned out to be of RRc type, while the remaining objects are of RRab type. Sixteen HST objects could not be confirmed with the OGLE data. It is worth noting that MiNDSTEp study (Figuera Jaimes *et al.* 2016) based on better resolution images and reaching more central parts of M54 confirmed variability of additional six HST objects: V212=VC35, V216=VC9, V221=VC8, V224=VC20, V225=VC37, and V232=VC41.

We also confirm classification of seven additional RR Lyr stars found by the MiNDSTEp consortium (Figuera Jaimes *et al.* 2016) and overlooked during our search: V218, V222, V235, V238, V243, V248, and V282.

Our search for new variable stars has led to the discovery of the following 83 objects: 26 RR Lyr-type stars, two Type II Cepheids, nine eclipsing binaries, two ellipsoidal binaries, 22 semi- or irregular variable red giants, and 22 unclassified variable stars. Among the RR Lyr variable stars, there are 18 RRab and eight RRc stars. *I*-band light curves of these new RR Lyr variable stars are shown in Figs. 6 and 7. In Fig. 8, we present light curves of all four Type II Cepheids. In addition to the two previously known BL Her-type stars (V1 and V2), we have discovered one more BL Her-type star (V230) and one W Vir-type star (V256). Among eclipsing binaries, we have found four EW systems and five EB systems. Light curves of eclipsing binary stars and semi-regular variable red giants are shown in Figs. 9 and 10, respectively. In the case of variable stars of unknown type, more data is required to properly classify them.

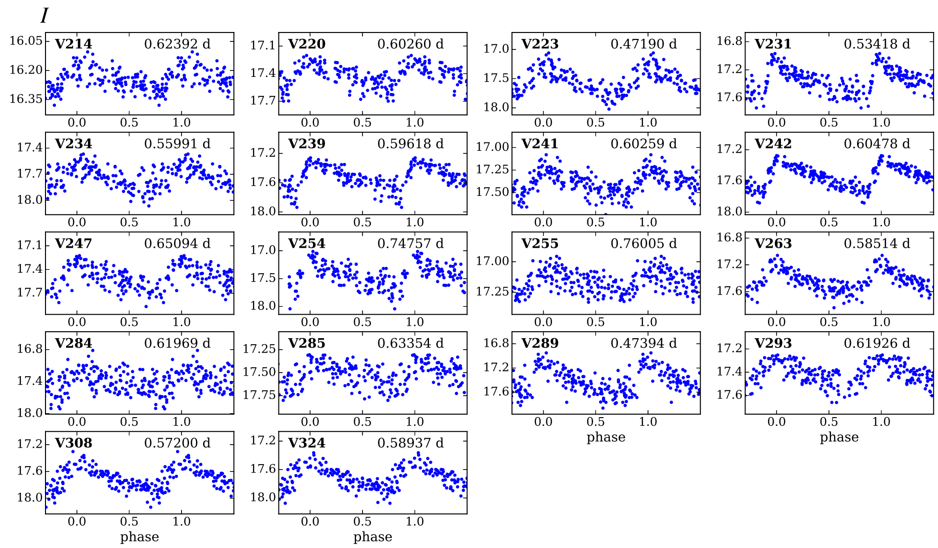


Fig. 6. Phased OGLE *I*-band light curves of new RRab variable stars from M54.

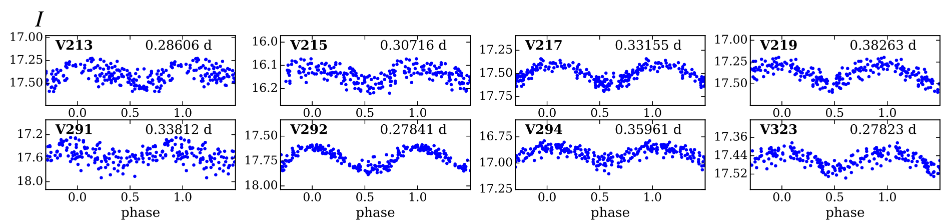


Fig. 7. Phased OGLE *I*-band light curves of new RRc variable stars from M54.

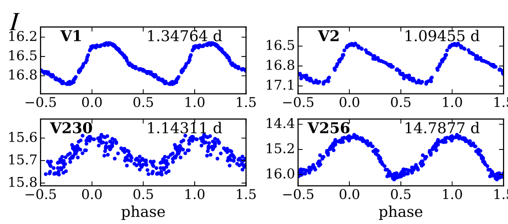


Fig. 8. Phased *I*-band light curves of all known Type II Cepheids in M54. Two bottom objects are newly discovered pulsators.

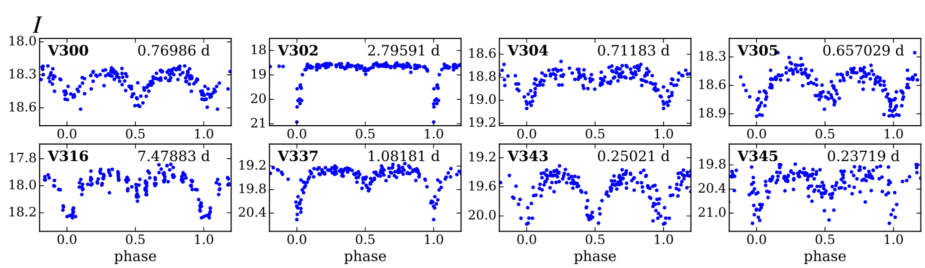


Fig. 9. Phased *I*-band light curves of selected eclipsing binary stars in the field of M54.

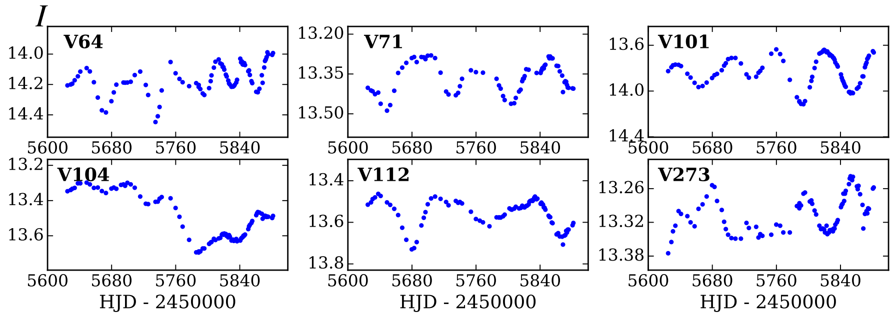


Fig. 10. *I*-band light curves of selected semi-regular variable red giants from M54 observed during 2011 season.

In the upper panel of Fig. 11, we present color–magnitude diagram (CMD) for the globular cluster M54 with positions of variable stars with measured brightness in the $V$ and $I$ bands. The background is formed of all stars detected within the tidal radius of the cluster with the OGLE standard pipeline. We only show variable stars located between the half-light and tidal radii. For comparison, in the lower panel of Fig. 11, we present CMD for a nearby off-cluster field containing mostly stars from the Sgr dSph galaxy. Common features are present in both diagrams. Foreground main sequence stars from the Galactic halo are seen in the area between $V-I=0.8$ mag and $V-I=0.9$ mag for $I<19.5$ mag. Red giants from the Galactic halo and Sgr dSph galaxy are spread along a wide arc from $(V-I,I)=(1.0,19.5)$ toward upper right corner. Sgr dSph red clump stars can be found around $(V-I,I)=(1.2,17.1)$. In the diagram for M54, there are additional features like prominent red giant branch with the red clump at $(V-I,I)=(1.15,17.0)$ and horizontal branch occupied by RR Lyr stars with $0.45<V-I<0.85$ mag. Note that the M54 red clump does not overlap with the Sgr dwarf red clump. The location of the M54 red clump slightly to the blue of the Sgr dSph red clump indicates that the cluster is more metal poor than the remaining body of the dwarf galaxy.

Based on measured brightness we confirm that the following RRab stars located between the half-light and tidal radii are not members of the globular cluster: V55, V65, V93, V119, and V121. We also confirm that RRab variable V92 is a field object despite its location at only 0.74 $r_{\rm h}$ from the center of M54. This star with a pulsation period 0.4847065(10) d is brighter than the M54 horizontal branch by about 0.35 mag. According to Clement *et al.* (2001) V92 is blended. Indeed, it has a neighbor of a similar brightness, but located about $1\farcs3$ (5 pix) away in OGLE images. At such distance the neighbor star cannot affect much the measured brightness of the variable.

The total number of RR Lyr stars considered as cluster members is 163. We assume that all variable stars within $r_h=0\farcm82$ but the mentioned V92 belong to M54. Based on brightness information given in Clement *et al.* (2001) we assume that RR Lyr variable stars V14, V30, V56, V75, which fell in the gaps between

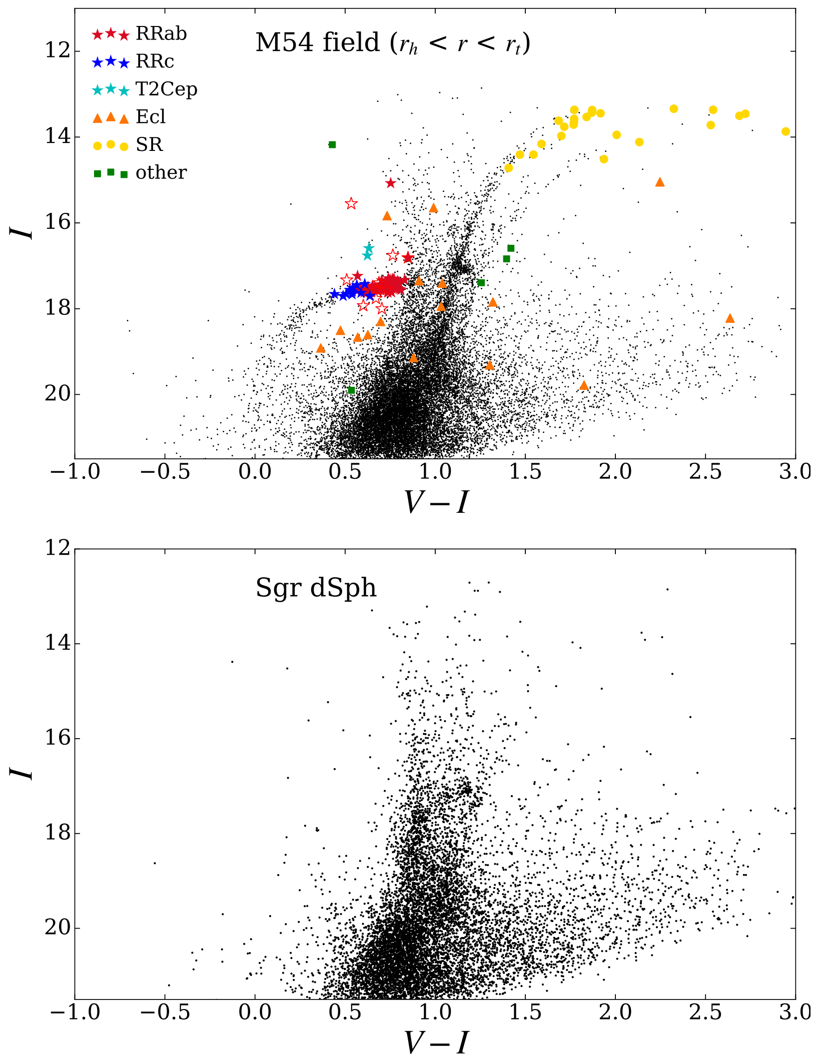


Fig. 11. $I$ *vs.* $V - I$ diagrams for the M54 cluster field (*upper panel*) and an off-cluster area (lower panel). The *upper panel* shows stars located between the half-light radius ($r_{\rm h} = 0\overset{\prime}{.}82$) and tidal radius ($r_{\rm t} = 7\overset{\prime}{.}5$) of the cluster. Variable stars of different types are marked with different symbols. Open red asterisks denote non-member RRab stars. The *lower panel* presents stars from the southern half of the OGLE-IV chip BLG708.09. Note the prominent features of M54 such as the red giant branch and horizontal branch. The M54 red clump can be found to the blue of the Sgr dSph red clump. This indicates a lower metallicity of the cluster in comparison to the parent dwarf galaxy.

the OGLE chips, belong to the cluster. Among the 163 members there are 133 RRab stars, 28 RRc stars, and 2 RRd stars. Fundamental-mode RR Lyr stars being non-members of M54 are marked with open circles on the map in Fig. 5.

The membership status of V184 requires a few words of explanation. This variable is located at 0.86 $r_{\rm h}$ from the center. Its pulsation period is 0.959234(8) d. It is much longer than the average for the cluster (0.599 d). V184 is brighter than the cluster horizontal branch by about 0.50 mag. We suppose that this object is an M54 RR Lyr star probably leaving the horizontal branch toward the asymptotic giant branch and crossing the instability strip. In future, it would be worth to verify whether its period increases due to its evolution redward across the instability strip. We mark this object with a filled yellow circle in Fig. 5.

Positions of Type II Cepheids V1 and V2 in the cluster CMD (Fig. 11) confirm that these stars are members of the cluster. The two newly discovered Type II Cepheids, BL Her-type variable V230 and W Vir-type variable V256, are located well within the half-light radius of M54, at $0.18\ r_{\rm h}$ and $0.12\ r_{\rm h}$, respectively. Their estimated mean *I*-band brightness is 15.67 mag and 15.29 mag, respectively. These facts clearly indicate that the two Cepheids also belong to the cluster.

Based on the position in the CMD, we conclude that probably all semi-regular variable red giants detected within the tidal radius of M54 are likely cluster members. Observed binary stars and other unclassified variable stars are likely foreground objects.

## 6. Distance to M54

Based on 71 RRab stars considered as members of M54 and located between its half-light and tidal radii to minimize the effect of crowding, and for which we have information on brightness in $V$ and $I$, we estimate the distance to this globular cluster. Using the presented sequence of Eqs.(1–9) we find $d_{\rm M54} = 26.7 \pm 0.03_{\rm stat}$ kpc. This is the median value of individual distances to these stars. The statistical uncertainty is calculated using error propagation formula applied to Eq.(8) assuming a mean accuracy of OGLE photometric measurements $\sigma_I = 0.02$ mag and a very small mean random error of $\phi_{31}$ of 0.018. Uncertainties of the pulsation periods are negligible. The final value of the statistical uncertainty was divided by square root of the number of used stars. The largest contributions to the total systematic uncertainty are errors of the zero point of the period–luminosity–metallicity relation (Eq. 3), the conversion for metallicity (Eq. 2), and uncertainty of the $E(B-V)$ map (Chen *et al.* 1999). The systematic error on distance modulus can be as large as 0.1 mag (Pietrukowicz *et al.* 2015), which at the distance of M54 translates to 1.3 kpc.

## 7. Multiple Old Populations in M54 and the Sgr dSph Stream

We use the detected RR Lyr stars to look for old stellar populations, both in the cluster and main body of the dwarf galaxy. In Fig. 12, we compare period distributions for all RRab stars from M54 and the Sgr stream. The mean period for all known cluster members is 0.599 d, not excluding the long-period variable V184. For a comparison, the mean period for the Sgr dwarf RRab stars is slightly lower, 0.579 d. We applied the Kolmogorov–Smirnov statistics to compare the distributions. We find the $p$-value below 1% which indicates that the distributions are almost identical.

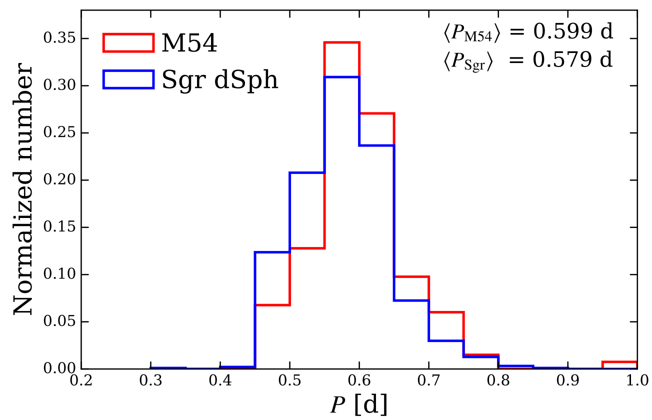


Fig. 12. Comparison of period distributions for RRab stars from the globular cluster M54 and Sgr dSph galaxy.

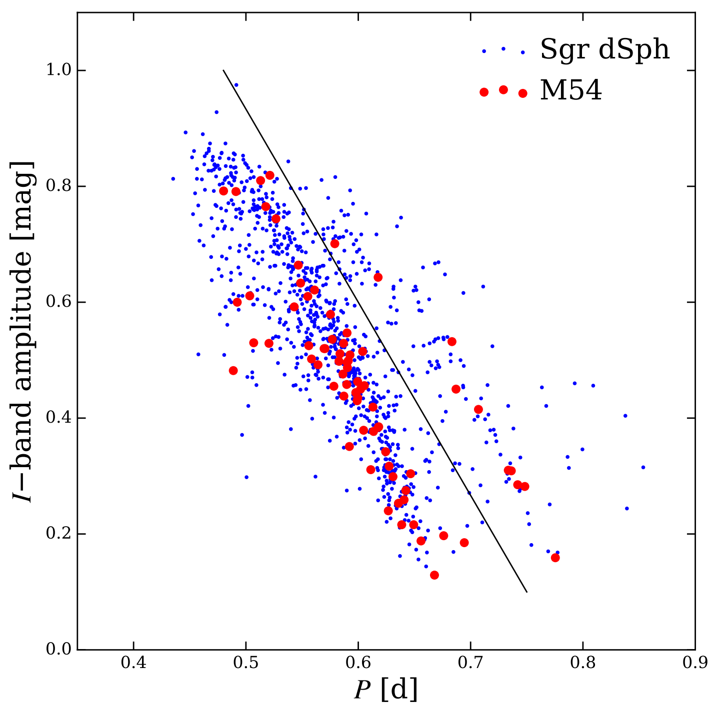


Fig. 13. Bailey diagram for RRab stars from M54 (red points) and main body of the Sgr dSph galaxy (blue points). Straight line roughly divides the variable stars into two Oosterhoff groups: OoI group at shorter periods and OoII at longer periods. Two sequences indicate the presence of two old populations both in the cluster and Sgr dwarf.

In Fig. 13, we plot period–amplitude (or Bailey) diagram for cluster and Sgr dSph galaxy fundamental-mode RR Lyr stars. To minimize the effect of crowding on the measured $I$-band amplitude we only show variable stars located between the

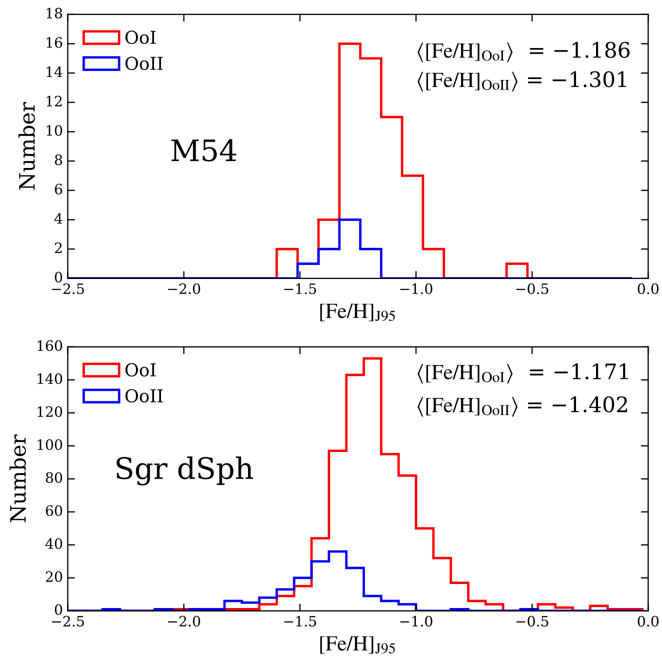


Fig. 14. Comparison of metallicity distributions for RRab stars representing two Oosterhoff groups from M54 (*upper panel*) and the Sgr dSph galaxy (*lower panel*). The metallicities are on the Jurcsik (1995) scale.

half-light and tidal radii of the cluster. In both systems, the cluster and dwarf galaxy, RRab stars form two sequences, which correspond to Oosterhoff groups OoI and OoII. Despite a low number of M54 RRab variable stars representing the OoII group (only ten), it is very unlikely that these objects are contaminants from the Sgr dwarf. This number of objects gives an average density of 0.057 $\mathrm{arcmin}^{-2}$ for the cluster. For a comparison, in the whole off-cluster area within the OGLE-IV field BLG708 covering $\approx 1.35$ $\mathrm{deg}^2$ there is about 30 such variable stars (*i.e.*, objects above the broader sequence in Fig. 13), which gives 0.006 $\mathrm{arcmin}^{-2}$ or roughly ten times lower density for the Sgr dwarf. Approximate ratio of detected OoII stars to OoI stars in the cluster and dwarf galaxy is very similar: 14% and 16%, respectively. This is roughly twice smaller to what was found in the Sgr dSph stream far away from the core (*e.g.*, Zinn *et al.* 2014). The observed bimodal Oostherhoff distribution in the dwarf galaxy and globular cluster indicates the presence of two metal-poor populations which differ by about 0.2 dex (Fig. 14): OoI of $[\mathrm{Fe/H}]_{\mathrm{J95}} \approx -1.2$ dex and OoII of $[\mathrm{Fe/H}]_{\mathrm{J95}} \approx -1.4$ dex. No bimodal distribution in the metal-poor regime has been found in spectroscopic surveys of red giants from M54 and Sgr nucleus (Bellazzini *et al.* 2008, Carretta *et al.* 2010), but they did not include RR Lyr stars at all. Similar ratios of OoII to OoI variable stars in the cluster and in the dwarf galaxy suggest the same formation scenario of both systems.

## 8. Conclusions

We presented the 3D picture of the Sgr dSph galaxy observed roughly in the background of the Galactic bulge based on RRab stars. We estimated the line-of-sight thickness of the central section of the Sgr dSph stream to be $\mathrm{FWHM}_{\mathrm{cen}} =$ 2.42 kpc. We also presented the results of our comprehensive search for variable stars in the field of the globular cluster M54 residing in the core of the Sagittarius Dwarf Spheroidal galaxy. Our aim was to verify and expand the existing list of variable stars in M54. We have confirmed the presence of 20 RR Lyr-type stars indicated in the archival HST/WFPC2 images by Montiel and Mighell (2010). We have discovered 83 new variable stars, 26 of which are RR Lyr stars. We have also reviewed the previously suggested variable stars, showing that 24 variable stars, mostly classified as of RR Lyr type, are in fact non-variable. Using RRab pulsators, we have estimated the distance to the M54 cluster obtaining $d_{\mathrm{M54}} = 26.7 \pm 0.03_{\mathrm{stat}} \pm 1.3_{\mathrm{sys}}$ kpc. We have confirmed the presence of two old populations, both in the cluster and dwarf galaxy.

**Acknowledgements.** We would like to thank Profs. M. Kubiak and G. Pietrzyński, former members of the OGLE team, for their contribution to the collection of the OGLE photometric data over the past years. We also thank Prof. V. Belokurov for discussion and suggestions and Drs. R. Figuera Jaimes and D. Bramich for informing us about MiNDSTEp consortium study of the M54 center and joint work on unambiguous numbering of newly discovered variable stars. We acknowledge the referee for very constructive comments.

The OGLE project has received funding from the National Science Centre, Poland, grant MAESTRO 2014/14/A/ST9/00121 to A.U. This work has been also supported by the Polish Ministry of Sciences and Higher Education grants No. IP2012 005672 under the Iuventus Plus program to P.P. and No. IdP2012 000162 under the Ideas Plus program to I.S.

## REFERENCES

Alard, C. 2001, *A&A*, **377**, 389.
Alcock, C., *et al.* 1997, *ApJ*, **474**, 217.
Bellazzini, M., *et al.* 2008, *AJ*, **136**, 1147.
Belokurov, V., *et al.* 2006, *ApJ*, **642**, L137.
Belokurov, V., *et al.* 2014, *MNRAS*, **437**, 116.
Carretta, E., *et al.* 2010, *A&A*, **520A**, 95.
Catelan, M., Pritzl B.J., and Smith, H.A. 2004, *ApJS*, **154**, 633.
Chen, B., Figueras, F., Torra, J., Jordi, C., Luri, X., and Galadí-Enríquez, D. 1999, *A&A*, **352**, 459.
Clement, C.M., *et al.* 2001, *AJ*, **122**, 2587.
Cseresnjes, P., Alard, C., and Guibert, J. 2000, *A&A*, **357**, 871.
Cseresnjes, P. 2001, *A&A*, **375**, 909.
Dolphin, A.E. 2000a, *PASP*, **112**, 1383.
Dolphin, A.E. 2000b, *PASP*, **112**, 1397.

Figuera Jaimes, R., *et al.* 2016, *A&A*, in press, arXiv:1605.06141.
Gonzalez, O.A., Rejkuba, M., Zoccali, M., Valenti, E., Minniti, D., Schultheis, M., Tobar, R., and Chen, B. 2012, *A&A*, **543A**, 13.
Harris, W.E. 1996, *AJ*, **112**, 1487.
Ibata, R.A., Gilmore, G., and Irwin, M.J. 1994, *Nature*, **370**, 194.
Jurcsik, J. 1995, *Acta Astron.*, **45**, 653.
Jurcsik, J., and Kovács, G. 1996, *A&A*, **312**, 111.
Kunder, A., and Chaboyer, B. 2009, *AJ*, **137**, 4478.
Layden, A.C., and Sarajedini, A. 1997, *ApJ*, **486**, L107.
Layden, A.C., and Sarajedini, A. 2000, *AJ*, **119**, 1760.
Majewski, S.R., Skrutskie, M.F., Weinberg, M.D., and Ostheimer, J.C. 2003, *ApJ*, **599**, 1082.
Mateo, M., Udalski, A., Szymański, M., Kaluzny, J., Kubiak, M., and Krzemiński, W. 1995a, *AJ*, **109**, 588.
Mateo, M., Kubiak, M., Szymański, M., Kaluzny, J., Krzemiński, W., and Udalski, A. 1995b, *AJ*, **110**, 1141.
Montiel, E.J., and Mighell, K.J. 2010, *AJ*, **140**, 1500.
Monaco, L., Bellazzini, M., Ferraro, F.R., and Pancino, E. 2004, *MNRAS*, **353**, 874.
Monaco, L., Bellazzini, M., Ferraro, F.R., and Pancino, E. 2005, *MNRAS*, **356**, 1396.
Mróz, P., *et al.* 2015, *Acta Astron.*, **65**, 313.
Nataf, D.M., *et al.* 2013, *ApJ*, **769**, 88.
Pietrukowicz, P. 2016, in: "The General Assembly of Galaxy Halos: Structure, Origin and Evolution", *IAUS Proceedings*, **317**, p. 116.
Pietrukowicz, P., *et al.* 2013, *Acta Astron.*, **811**, 12.
Pietrukowicz, P., *et al.* 2015, *ApJ*, **811**, 113.
Rosino, L. 1952, *Memorie della Societá Astronomia Italiana*, **23**, 49.
Rosino, L., and Nobili, F. 1958, *Memorie della Societá Astronomia Italiana*, **29**, 413.
Sarajedini, A., and Layden, A.C. 1995, *AJ*, **109**, 1086.
Schwarzenberg-Czerny, A. 1996, *ApJ*, **460**, L107.
Schechter, P.L., Mateo, M, and Saha, A. 1993, *PASP*, **105**, 1342.
Schlafly, E.F., and Finkbeiner, D.P. 2011, *ApJ*, **737**, 103.
Schlegel, D.J., Finkbeiner, D.P., and Davis, M. 1998, *ApJ*, **500**, 525.
Smolec, R. 2005, *Acta Astron.*, **55**, 59.
Sollima, A., Cacciari, C., Bellazzini, M., and Colucci, S. 2010, *MNRAS*, **406**, 329.
Soszyński, I., *et al.* 2013, *Acta Astron.*, **63**, 21.
Soszyński, I., *et al.* 2014, *Acta Astron.*, **64**, 177.
Soszyński, I., *et al.* 2015, *Acta Astron.*, **65**, 297.
Torrealba, G., *et al.* 2015, *MNRAS*, **446**, 2251.
Udalski, A., Szymański, M. K., and Szymański, G. 2015, *Acta Astron.*, **65**, 1.
Zinn, R., Horowitz, B., Vivas, A. K., Baltay, C., Ellman, N., Hadjiyska, E., Rabinowitz, D., and Miller, L. 2014, *ApJ*, **781**, 22.